

## A Q-switched Ho:YAG laser assisted nanosecond time-resolved T-jump transient mid-IR absorbance spectroscopy with high sensitivity

Deyong Li, Yunliang Li, Hao Li, Xianyou Wu, Qingxu Yu, and Yuxiang Weng

Citation: *Review of Scientific Instruments* **86**, 053105 (2015); doi: 10.1063/1.4921473

View online: <http://dx.doi.org/10.1063/1.4921473>

View Table of Contents: <http://scitation.aip.org/content/aip/journal/rsi/86/5?ver=pdfcov>

Published by the [AIP Publishing](#)

---

### Articles you may be interested in

[High average power passively Q-switched laser diode side-pumped green laser by using Nd:YAG/Cr4+:YAG/YAG composite crystal](#)

*J. Laser Appl.* **26**, 032009 (2014); 10.2351/1.4870435

[Cr:Er:Tm:Ho:yttrium aluminum garnet laser exhibiting dual wavelength lasing at 2.1 and 2.9  \$\mu\text{m}\$ : Spectroscopy and laser performance](#)

*J. Appl. Phys.* **91**, 11 (2002); 10.1063/1.1419211

[Design and implementation of a rapid-mixer flow cell for time-resolved infrared microspectroscopy](#)

*Rev. Sci. Instrum.* **71**, 4057 (2000); 10.1063/1.1319342

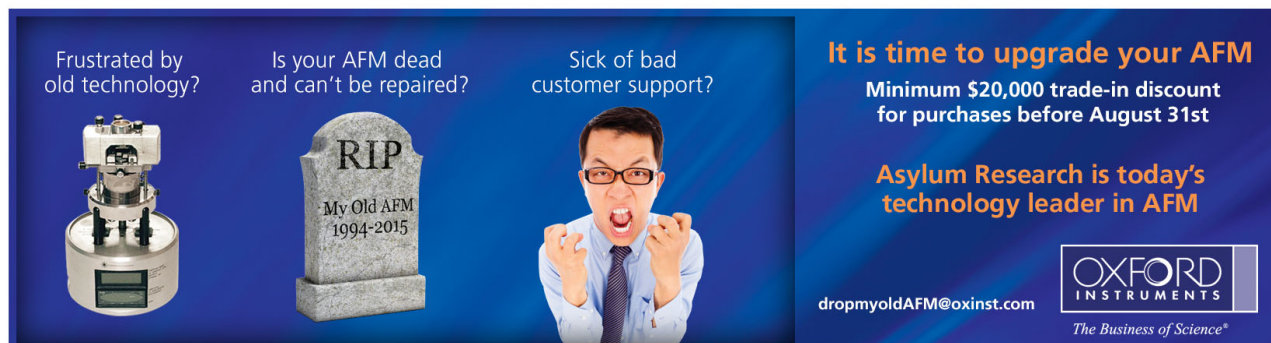
[Studies on the mechanism of the Sarcoplasmic Reticulum Ca<sup>2+</sup>-ATPase using time-resolved FTIR-spectroscopy](#)

*AIP Conf. Proc.* **430**, 358 (1998); 10.1063/1.55836

[A modified stopped-flow apparatus for time-resolved protein phosphorescence](#)

*Rev. Sci. Instrum.* **68**, 4583 (1997); 10.1063/1.1148435

---



Frustrated by old technology?

Is your AFM dead and can't be repaired?

Sick of bad customer support?

**It is time to upgrade your AFM**

Minimum \$20,000 trade-in discount for purchases before August 31st

Asylum Research is today's technology leader in AFM

dropmyoldAFM@oxinst.com

**OXFORD**  
INSTRUMENTS  
*The Business of Science®*

# A Q-switched Ho:YAG laser assisted nanosecond time-resolved T-jump transient mid-IR absorbance spectroscopy with high sensitivity

Deyong Li,<sup>1</sup> Yunliang Li,<sup>1</sup> Hao Li,<sup>1</sup> Xianyou Wu,<sup>2</sup> Qingxu Yu,<sup>3</sup> and Yuxiang Weng<sup>1,a)</sup>

<sup>1</sup>Key Laboratory of Soft Matter Physics, Institute of Physics, Chinese Academy of Sciences, Beijing 100190, China

<sup>2</sup>Anhui Institute of Optics and Fine Mechanics, Chinese Academy of Sciences, Hefei 230031, China

<sup>3</sup>School of Physics and Optoelectronic Technology, Dalian University of Technology, No. 2, Linggong Road, Dalian 116023, China

(Received 15 February 2015; accepted 10 May 2015; published online 27 May 2015)

Knowledge of dynamical structure of protein is an important clue to understand its biological function *in vivo*. Temperature-jump (T-jump) time-resolved transient mid-IR absorbance spectroscopy is a powerful tool in elucidating the protein dynamical structures and the folding/unfolding kinetics of proteins in solution. A home-built setup of T-jump time-resolved transient mid-IR absorbance spectroscopy with high sensitivity is developed, which is composed of a Q-switched Cr, Tm, Ho:YAG laser with an output wavelength at 2.09  $\mu\text{m}$  as the T-jump heating source, and a continuous working CO laser tunable from 1580 to 1980  $\text{cm}^{-1}$  as the IR probe. The results demonstrate that this system has a sensitivity of  $1 \times 10^{-4}$   $\Delta\text{OD}$  for a single wavelength detection, and  $2 \times 10^{-4}$   $\Delta\text{OD}$  for spectral detection in amide I' region, as well as a temporal resolution of 20 ns. Moreover, the data quality coming from the CO laser is comparable to the one using the commercial quantum cascade laser. © 2015 AIP Publishing LLC. [<http://dx.doi.org/10.1063/1.4921473>]

## I. INTRODUCTION

Static structure of protein is a key factor in understanding the biological functions of proteins.<sup>1</sup> However, this static information is definitely not enough since protein structures would change when realizing its biological functions *in vivo*.<sup>2</sup> For obtaining protein dynamical structures, various time-resolved methods have been developed, such as nuclear magnetic resonance (NMR),<sup>3</sup> X-ray scattering,<sup>4</sup> single molecular fluorescence resonance energy transfer (FRET),<sup>5</sup> fluorescence,<sup>6</sup> circular dichroism (CD),<sup>7</sup> and mid-IR absorption spectroscopy.<sup>8</sup> For most of the proteins, about 75% of early folding events would complete in less than 1 ms, and folding/unfolding of the secondary structures can be as fast as ns.<sup>9</sup> Therefore, fast trigger for inducing the protein structural changes is imperative in all the detection methods.

Among the various methods as aforementioned, it has been shown that time-resolved temperature-jump (T-jump) transient mid-IR absorbance spectroscopy is a powerful tool in investigating the protein folding/unfolding kinetics as well as the protein dynamical structures.<sup>10–12</sup> This method has been successfully employed to reveal the peculiar biological functions correlated to the protein structural changes in a number of large protein molecules under biological conditions,<sup>13–15</sup> protein-protein interactions,<sup>16</sup> and protein conformation and biochemical process related disease.<sup>17</sup>

With the T-jump method, the sudden change in protein structure is realized by displacement of the native protein structure at room temperature to an unfolded or partially unfolded states by a rapid temperature change, which is induced by heating the solvent ( $\text{H}_2\text{O}$  or  $\text{D}_2\text{O}$ ) with a

nanosecond near IR laser pulse.<sup>18</sup> Then, the evolution of protein dynamical conformation is monitored with another continuous working (cw) mid-IR laser tracing the spectral fingerprints of protein secondary structure in amide I or amid I' (the prime denotes deuteriated proteins) region.<sup>19</sup> Compared to the other methods for fast initiation of a protein structural change, such as stopped-flow<sup>20</sup> and laser induced chemical reactions,<sup>21</sup> laser-induced T-jump is realized via the absorption of the pulsed energy by the solvent or alternatively by dye. Among all these methods, T-jump induced by directly heating the solvent has two obvious advantages of (1) high temporal resolution and (2) no chemical contaminants such as protein denaturants involving fast mixing in stopped-flow<sup>22</sup> or photoactive chemicals in laser induced chemical reactions.

The technique of T-jump was pioneered by Eigen and Hammes on heating the solution with rapid capacitance discharge.<sup>23</sup> Since then, various other methods including resistive heating,<sup>24</sup> microwave absorption,<sup>25</sup> and the visible or ultraviolet light from flash lamp<sup>26</sup> have been employed to reduce the rising time of the T-jump as well as to increase the amplitude of the T-jump; however, the T-jump response time was limited in  $\mu\text{s}$  scale. With the advent of shorter pulse duration from Q-switched laser, T-jump response time in an order of nanosecond has been achieved.<sup>27</sup>

One more side, in the study of the protein dynamical structures, the samples are always prepared in the solvent of  $\text{H}_2\text{O}$  or  $\text{D}_2\text{O}$ , so the effective wavelength for heating this solution has to be considered. While this cannot be achieved with the fundamental output wavelength at 1.064  $\mu\text{m}$  of a most commonly used nanosecond pulsed Q-switched Nd:YAG laser (repetition rate 10 Hz, pulse width 10 ns), this fundamental frequency has to be converted to a frequency to match overtone frequencies of O–H or O–D stretching vibrations in  $\text{H}_2\text{O}$  or  $\text{D}_2\text{O}$ .<sup>27</sup> A suitable overtone wavelength

<sup>a)</sup>Electronic mail: yxweng@iphy.ac.cn

of H<sub>2</sub>O is around 1.54  $\mu\text{m}$  and 1.9  $\mu\text{m}$  for D<sub>2</sub>O. For mid-IR probe of amide I' band, D<sub>2</sub>O is generally used instead of H<sub>2</sub>O, for the former can provide a spectral window in the amide I' region. Several frequency shifting methods have been employed, e.g., Raman frequency converter which can shift 1.064  $\mu\text{m}$  to 1.54  $\mu\text{m}$  by choosing the gas medium as CH<sub>4</sub> or to 1.9  $\mu\text{m}$  as with a medium of H<sub>2</sub>.<sup>18,28</sup> Our own experience of using the Raman frequency converter shows that there exists a certain spatial drift of the output beam possibly due to the inefficient heat dumping inside the cell or high pump energy, which would significantly affect the shot-to-shot spatial reproducibility as also noted by the other groups.<sup>27</sup> Other method such as difference frequency generation (DFG) in a nonlinear optical crystal between a dye laser and the fundamental output wavelength of the Q-switched laser has also been employed to produce a heating pulse at 1.9  $\mu\text{m}$ ,<sup>29</sup> but the output energy of this method is limited by the DFG efficiency. Later, optical parametric oscillator (OPO) has been used to shift the 1.064 to 1.570  $\mu\text{m}$ .<sup>30</sup> An OPO with output wavelength tunable from 1.80 to 2.05  $\mu\text{m}$  has been reported, which employed a Q-switched Nd:YLF laser (10 ns pulses) with a 1 kHz repetition rate to pump a potassium titanyl arsenate (KTA), producing 1 mJ pulses with a shot-to-shot pulse stability as high as 98%.<sup>31</sup> However, the 1 ms duration time between the two successive pulses is much less than the cooling time for the heated sample by a single pulse. Effort has been devoted to construction of an OPO with low repetition rate (10 Hz), which results in an output energy fluctuation range (from minimum to maximum) being as large as 40%. This limits it as a heating laser for high sensitivity detection.<sup>32</sup> Holmium yttrium-lithium-fluoride (YLF) laser which can directly deliver a fundamental wavelength of 2.065  $\mu\text{m}$  has been designed for T-jump;<sup>33</sup> however, the pulse width of the laser is as long as 260  $\mu\text{s}$ . Therefore, it would be ideal for the T-jump study to develop a Q-switched laser as the heating source with an output wavelength around 2  $\mu\text{m}$ , a pulse duration around nanoseconds, a low repetition rate, and high stability both in energy and spatial modes.

In the measurement of protein dynamical structure, generally a 50- $\mu\text{m}$  sample cell is used, the inhomogeneity in the jumped temperature between the front and back surfaces of the D<sub>2</sub>O liquid is less than 10% when pumped at 1.9  $\mu\text{m}$  (the absorption coefficient for D<sub>2</sub>O at 1.907  $\mu\text{m}$  is 13.9  $\text{cm}^{-1}$ ),<sup>8,34</sup> and the concentration of the protein samples is kept as about

10 mg/ml for achieving a difference absorbance about several mOD at a T-jump about 10–20 °C. This sets a pre-requirement for the apparatus with a sensitivity at least about 1 mOD for acquisition of a reliable difference spectrum. What is more, in many protein studies, the concentration is much lower than 10 mg/ml, which demands a much higher detection sensitivity. Therefore, in addition to an appropriate heating laser, a T-jump time-resolved difference mid-IR spectrometer suitable for successful study of protein dynamical structures also relies on a stable, enough output power, and tunable mid IR laser as the probe source.

In early time, cw lead salt infrared diode lasers were used as the probe which is tunable from 1600 to 1700  $\text{cm}^{-1}$  covering the amide I' region.<sup>8,11</sup> Although the transient difference IR spectra covering the whole amide I' region have scarcely reported, it has been realized in our group with the development of a CO gas laser.<sup>13,15,35,36</sup> Recently, the advent of quantum cascade laser (QCL) in mid IR region with a broader tuning range and higher power provides a better IR probe source to replace lead salt infrared diode lasers.<sup>37,38</sup> Besides, other time-resolved broad band mid IR spectroscopic methods have also been reported including step-scan FTIR,<sup>39</sup> broad band fs IR pulse probe,<sup>40</sup> and 2D IR spectrum<sup>41</sup> coupled to T-jump.

As we have noted, in all the reported single wavelength detections by tuning the IR source in T-jump experiments, the sensitivity is wavelength dependent and it generally exceeds 1 m $\Delta$ OD. In this work, by optimizing the home-built cw CO laser and a home-built Cr, Tm, Ho:YAG laser, a laser induced T-jump infrared setup with a single wavelength detection sensitivity of  $10^{-4}$   $\Delta$ OD and spectral detection sensitivity of  $2 \times 10^{-4}$   $\Delta$ OD in amide I' region is provided. Finally, the performance of CO laser was further compared to that of QCL for cytochrome c (cyt c) in 100 mM KCl solution, and the results show that the transient signals from both the IR sources are similar and comparable.

## II. EXPERIMENTAL SETUP

The layout of our T-jump time-resolved mid-IR difference absorbance spectrometer is shown in Fig. 1, which has been greatly improved.<sup>42</sup> It consists of a home-built Q-switched Cr, Tm, Ho:YAG laser, a home-built cw CO mid-IR laser, or alternatively, a QCL (Day light company), water-circulated sample cell, and a detection system. Explicitly, the

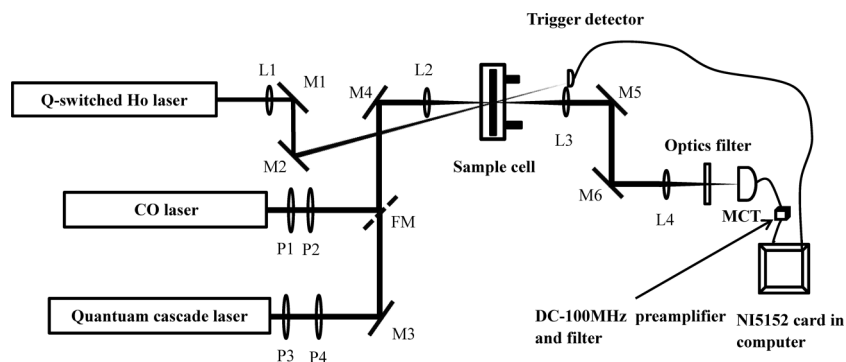


FIG. 1. The layout of T-jump time-resolved mid-IR difference absorbance spectrometer. M1–M6: Au-coated mirror; L1–L4: CaF<sub>2</sub>,  $f = 50$  mm; FM: flip mirror; and P1–P4: rotatable mid-IR polarizer.

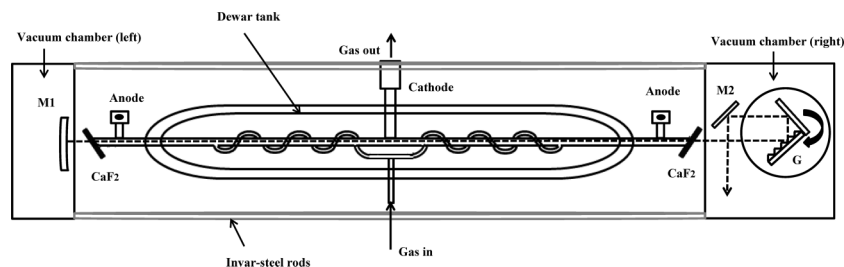


FIG. 2. Schematic diagram of the home-built CO laser. M1: concave Au-coated mirror ( $R = 5$  m); M2: Au-coated mirror; and G: aluminum grating with 150 grooves/mm.

IR probe beam was detected by a liquid nitrogen cooled photovoltaic MCT detector (Kolmar, Newburyport, MA), which is connected to a 500 MHz low-pass band filter and a sensitive current preamplifier (Kolmar, KA020-A1, bandwidth 100 MHz). The intensity of the transmitted IR probe beam was recorded by an 8-bit data acquisition card (NI5152, National Instruments). The signals were finally transferred to a PC for data record and analysis.

### A. Continuous wave CO laser

A home-built liquid nitrogen cooled cw CO laser is schematically illustrated in Fig. 2. The laser cavity has a length of 165 cm, consisting of one total reflective concave end gold mirror (M1) (Radius = 5 m, reflectivity above 98%) and the output coupling element is an aluminum grating (G) with 150 grooves/mm. This grating works in the Littrow configuration, namely, the light in the first order of the diffraction is reflected back to the laser cavity for the laser oscillations, and the output laser is through zero-order diffraction. When the grating is tuned for different output wavelengths, the output beam along the direction of zero-order diffraction can always be fixed in the same direction. Selection of the output wavelength is realized by rotating the grating sitting on the turret which is controlled by a remote computer. And the zero-order diffracted output beam is steered by a flat reflective gold mirror M2. The end mirror and the grating turret are placed in two vacuum chambers, respectively; the vacuum chambers prevent the vapor getting into the cavity, as well as keeping away the interference from the environment such as sound which would insert a mechanical vibration on the end mirrors. The two chambers were mechanically held at four corners of a side-wall facing the laser cavity by four Invar-steel rods which have a very small thermal expansion coefficient. To minimize the thermal perturbation from the environment induced by the evaporation of the liquid  $N_2$ , the Invar-steel rods are electrically heated to  $32^\circ\text{C}$ . The discharge tube is immersed in liquid  $N_2$  filled in a Dewar tank made of fused silica during operation. The Dewar tank is supported on an iron base plate without any connection to the Invar rods. All these measures taken above greatly enhance the stability of the output laser. Figure 3 presents a typical short-term power stability curve in a time scale of 20 ms, which has a standard deviation of  $5.6 \times 10^{-4}$ , and we set the short-term power stability as 0.1%, while the long-term power stability is about 10% measured in hours. However, only the short-term power stability that matters in the transient absorption measurement.

The two ends of the discharge tube are sealed with two  $\text{CaF}_2$  plates aligned in a Brewster angle ( $36.3^\circ$ ). The spectral transmission range of  $\text{CaF}_2$  window sets a limit on the output wavelength of the CO laser at the red side. The final output wavelength can be continuously tuned from  $5.1 \mu\text{m}$  ( $1980 \text{ cm}^{-1}$ ) to  $6.3 \mu\text{m}$  ( $1580 \text{ cm}^{-1}$ ). A single output wavelength can be selected within the CO vibration-rotation spectrum with an approximate spectral spacing of  $4 \text{ cm}^{-1}$ , and the output wavelength was calibrated by an IR monochromator within an uncertainty of  $2 \text{ cm}^{-1}$ . We have also tried in using ZnSe plates as the sealing windows, and the output wavelength can reach as far as  $8.1 \mu\text{m}$  ( $1234 \text{ cm}^{-1}$ ); however, the ZnSe flat surface can easily be etched by ozone inside the tube, which is produced during the discharge process. The feeding gas inside the tube is a mixture of CO,  $N_2$ , He, and air at an appropriate ratio depending on the desired wavelength range. The stable flow of the working gases is kept at a pressure of 26.5 Torr and discharged with a high voltage. The IR laser has a TEM<sub>00</sub> mode with an average output power at a single wavelength around 20 mW for the minimum and 500 mW for the maximum, which is variable with the wavelength. Compared to the widely used diode laser IR probe source, the CO laser has advantages of much higher output power, wider tunable range, and a better beam quality, rendering itself an excellent probe source for studying the T-jump-induced protein secondary structural changes in the amide I ( $I'$ ) region.

### B. Q-switched Cr, Tm, Ho:YAG laser for T-jump

As we have shown, a pulsed laser with an output wavelength around  $2 \mu\text{m}$  would be an ideal heating source

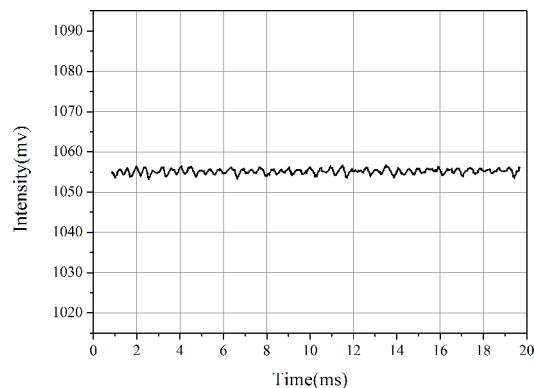


FIG. 3. Power stability of the CO laser in 20 ms time scale.



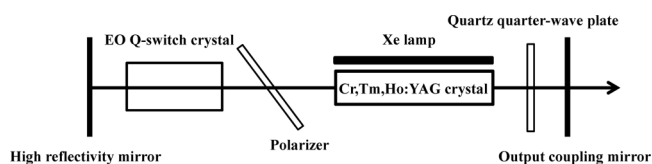


FIG. 4. Schematic diagram of the home-built Q-switched Ho:YAG laser.

to induce a T-jump in  $D_2O$ . Because of the lack of a proper Q-switch crystal, design and construction of a Q-switched laser operating at this wavelength with a nanosecond-pulse width and a high and stable energy output has always been a challenging task. Figure 4 shows a schematic diagram for a home-built electro-optically Q-switched Cr, Tm, Ho:YAG laser with an output wavelength at  $2.09 \mu\text{m}$  in our laboratory. The detail has been described elsewhere.<sup>43</sup>

Briefly, a 400 mm resonant cavity is constituted by a high reflective plane mirror (99% reflection) and a coupling mirror (70% transmission). A Cr, Tm, Ho:YAG crystal with a diameter of 5 mm and a length of 127 mm is used as the gain medium, which is doped with 1.5% Cr, 5.8% Tm, and 0.35% Ho. The laser crystal is pumped by one xenon lamp and is cooled by a chiller to a temperature of  $9^\circ\text{C}$ . A quartz quarter-wave plate is utilized to offset the thermal depolarization effect. An  $\text{Al}_2\text{O}_3$  plate polarizer with Brewster angle is placed in the cavity for controlling the polarization of the beam. A z-cut  $\text{La}_3\text{GaSiO}_{14}$  (LGS) crystal with a size of  $7 \text{ mm} \times 7 \text{ mm} \times 45 \text{ mm}$  is used for Q-switching inside the cavity. Under the high pumping flux, the thermal depolarization would seriously affect the uniformity of the beam pattern and output energy, but this can be compensated by twisting the quarter-wave plate located between the laser rod and the output coupling mirror. By optimizing the laser system, the final output laser pulse has a pulse duration of 50 ns, output wavelength at  $2.09 \mu\text{m}$ , 20 mJ output energy at 3 Hz repetition rate, and a shot-to-shot energy stability of  $\pm 1\%$ .

### C. Sample preparation

Horse heart cyt c (c-7752) was purchased from Sigma Aldrich without further purification.  $D_2O$  was obtained from Beijing Chemical Factory with a purity of 99.9%. In the T-jump measurement, the sample concentration was 1 mM (12.5 mg/ml). The sample and reference  $D_2O$  were sealed in a dual-compartment sample cell composed of two  $\text{CaF}_2$  windows, where a  $50\text{-}\mu\text{m}$  thick Teflon spacer with two isolated compartments was sandwiched. Deuteration of cyt c in  $D_2O$  was realized through the centrifugation-resuspension cycle with a membrane filter for protein, and was handled under a  $\text{N}_2$  atmosphere to eliminate contamination from humid air. All the other procedures for sample preparation and filling were kept in a dried air box with a humidity as low as less than 1%. During the measurements for signal from the sample and reference  $D_2O$ , the sample cell is only needed to be alternatively rotated between these two compartments, which can keep the sample and  $D_2O$  located in the same focal position of the pump and probe beams.

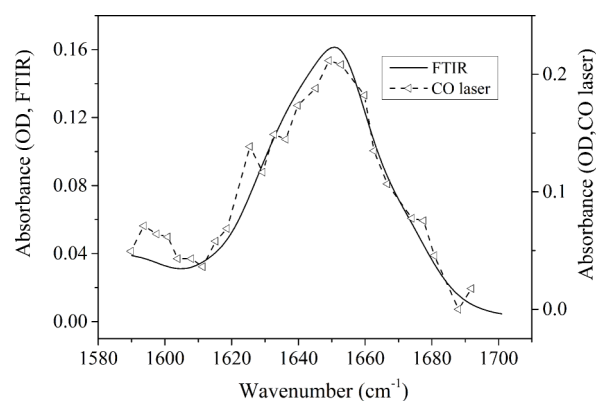


FIG. 5. Absorption spectra of cyt c measured using FTIR (solid line) and CO laser (triangles).

### D. Data collection

CO laser was optimized in the range of  $1600\text{--}1700 \text{ cm}^{-1}$ , and a steady-state IR absorption spectrum of cyt c in amide I' region was acquired by measuring the absorbance wavelength by wavelength in the ambient air. This absorption spectrum is compared to that collected in the vacuum by a FTIR spectrometer (VERTEX 70 V, Bruker Optics, DE) as shown in Fig. 5. The comparison of the IR absorption spectrum measured with CO laser with that of FTIR is used to show the reliability of the CO laser in the spectral measurement as well as to use FTIR spectrum to further calibrate the output wavelength of the CO laser. In this way, the reliability of the CO laser in the spectral measurement is confirmed and the uncertainty introduced during the calibration of the CO output wavelength can be further ruled out. However, the result shows that the IR absorption spectrum acquired with the CO laser is noisier. This can be owing to the facts that (1) the CO laser is a gas laser and its stability in hours cannot be comparable to that of the IR source of FTIR spectrometer and (2) the interference in absorbance measurement comes from the vapor absorption in the ambient air.

The probe beam from CO laser and the pump beam from Cr, Tm, Ho:YAG laser were focused at the same position in pump-probe beam geometry with  $100 \mu\text{m}$  and 1 mm spot size, respectively; their intensity can be separately controlled by adjusting the combination of a polarizer and a half-wave plate. Here, the spot size of the pump beam is purposely set much larger to avoid the photo-acoustic cavitation effects.<sup>44</sup>

## III. RESULTS AND DATA DISCUSSION

### A. Determination of signal-to-noise (S/N) ratio

For determining the S/N ratio, the sample and reference compartments in the sample cell were all filled with  $D_2O$ . The transient absorbance dynamics at a typical wavelength at  $1650 \text{ cm}^{-1}$  induced by T-jump for  $D_2O$  for both the sample and the reference were recorded in 100 laser shots, respectively, as illustrated in Fig. 6(a). The difference between these two transient absorbance dynamics can be found in Fig. 6(b). The fluctuation of the difference between these two kinetics is mainly distributed between  $\pm 10^{-4} \Delta\text{OD}$ , further improvement

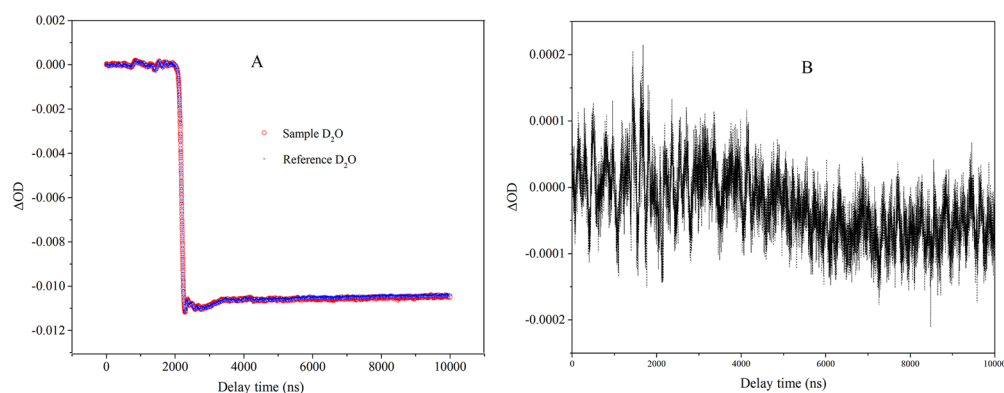


FIG. 6. Two transient absorbance kinetics of  $D_2O$  detected at  $1650\text{ cm}^{-1}$  denoted as from the sample and reference, respectively (a), and the corresponding difference kinetics (b).

is limited by the resolution of 8 bit data collection card. Therefore, the S/N ratio for the single wavelength detection can be as good as  $10^{-4}$   $\Delta OD$ .

## B. T-jump induced transient IR absorbance spectrum

In our current setup, the absorbance difference spectrum is constructed by every single wavelength detection. Thus during the measurement, the optical paths and the corresponding configuration may change slightly. This indicates that the spectral sensitivity in the amide I' region would be worse than that of a single wavelength detection. To examine the spectral sensitivity of the current apparatus, a previous studied sample cyt c was chosen as the reference.<sup>35</sup> The T-jump-induced difference absorbance spectrum of cyt c was acquired at room temperature ( $25^\circ\text{C}$ ) with a  $\Delta T = 10^\circ\text{C}$ . The corresponding T-jump induced transient IR absorbance spectrum of cyt c at  $2\ \mu\text{s}$  delay after the laser pulse (labeled as triangles) is shown in Fig. 7. The steady-state difference IR spectrum of the same sample between  $35^\circ\text{C}$  and  $25^\circ\text{C}$  (marked as the solid line) is also plotted for comparison.

It can be seen that the transient spectrum roughly follows that of the steady-state difference spectrum, but has a better peak resolution, e.g., the peaks at  $1630$ ,  $1645$ ,  $1662\text{ cm}^{-1}$ , and  $1682\text{ cm}^{-1}$  are clearly resolved in the transient difference

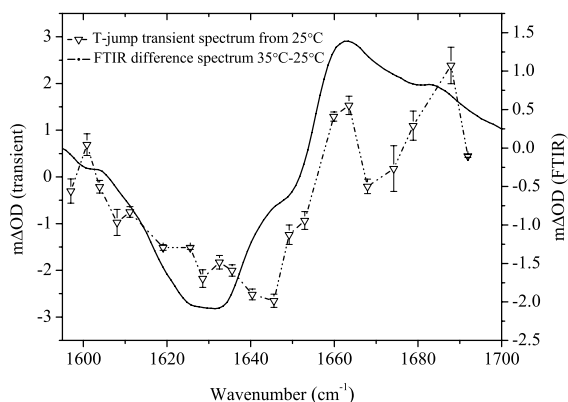


FIG. 7. T-jump induced difference absorbance spectrum (triangle) of cyt c in  $D_2O$  at room temperature ( $25^\circ\text{C}$ ) recorded at  $2\ \mu\text{s}$  after the pump laser and the steady-state difference IR spectrum (solid line) of cyt c between  $35^\circ\text{C}$  and  $25^\circ\text{C}$ .

absorbance spectrum, which embodies the secondary structural changes of cyt c during the unfolding process being induced by the T-jump. The transient absorption spectrum is obtained by averaging three independent measurements of the same sample with an error bar, i.e., independent tuning the wavelength in each measurement. The spectral sensitivity is defined as the averaged uncertainty for all the detecting wavelengths, which gives a value of  $\pm 2 \times 10^{-4}$   $\Delta OD$ .

Figure 8 plots a pair of transient kinetics acquired at  $1662$  and  $1630\text{ cm}^{-1}$ , together with an instrumental response curve. The instrumental response time constant is fitted as  $94\text{ ns}$  shown in the inset of Fig. 8. After deconvolution of the instrumental response time, these two kinetics can be fitted with a monoexponential decay of  $56$  and  $58\text{ ns}$ , respectively. The temporal resolution of the current setup is estimated to be  $20\text{ ns}$  after deconvolution.

To provide a direct comparison of the T-jump transient absorption spectra acquired with CO laser and commercial quantum cascade laser, the transient absorption spectra of cyt c in  $100\text{ mM KCl}$  solution were acquired with CO laser and QCL, respectively, shown in Fig. 9. The results show that the tendency is the same with a little different in details. Since the absorbance difference signal in pump-probe strongly depends on the overlap of the pump and the probe beams within the sample cell, the focal size of CO laser and QCL in sample cell cannot be kept exactly the same. Especially, due to the short

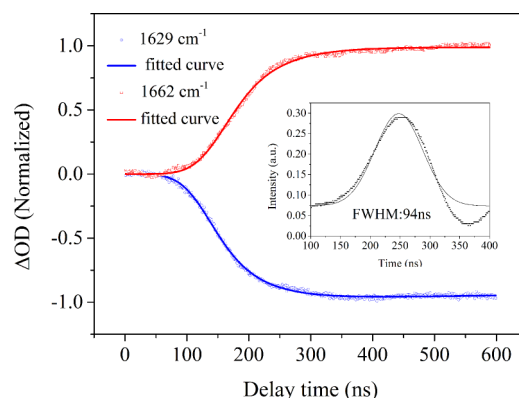


FIG. 8. Transient kinetics acquired at  $1662\text{ cm}^{-1}$  (red) and  $1630\text{ cm}^{-1}$  (blue). Inset: instrumental response curve of the transient mid-IR absorbance spectroscopy.

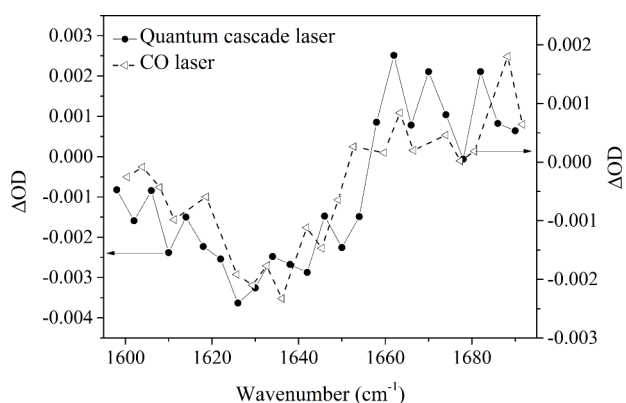


FIG. 9. The transient absorption spectra of cyt c in 100 mM KCl solution acquired with CO laser (open triangles) and QCL (solid cycles).

cavity of the QCL, the laser beam of different wavelength has a different divergence angle which would lead to different focal size in sample cell. What is more, the wavelength of the CO laser and QCL cannot be exactly matched, which will also influence the relative amplitude of the signal. This would account for the difference in detail between the two sets of the transient spectra. Consequently, the same tendency of the difference spectra acquired with these two different IR probe sources indicates that our system can provide a reliable option in the measurements of protein dynamical structure with T-jump technique.

#### IV. SUMMARY

With home-built cw CO laser as the IR probe and Cr, Tm, Ho:YAG laser as the T-jump trigger source, a T-jump transient IR difference absorbance spectroscopy has a sensitivity of  $1 \times 10^{-4}$   $\Delta OD$  for single wavelength detection and of  $2 \times 10^{-4}$   $\Delta OD$  for spectral detection in amide I', and a temporal resolution of 20 ns has been constructed. The data quality of this apparatus, when using cw CO laser, is comparable with using QCL as the IR probe source. Our results show that the Cr, Tm, Ho:YAG laser provides a heating source with a good beam quality and stability either in spatial mode or output energy. The high sensitivity of the instrument will be a useful tool in the future study of protein dynamical structures.

#### ACKNOWLEDGMENTS

This work is supported by Chinese Academy of Sciences Instrumental Development Program (YZ200842) and the Natural Science Foundation of China (Grant No. 21433014).

<sup>1</sup>J. H. Dawson, *Science* **240**, 433 (1988).

<sup>2</sup>F. G. Parak, *Curr. Opin. Struct. Biol.* **13**, 552 (2003).

<sup>3</sup>G. Navon, Y. Q. Song, T. Room, S. Appelt, R. E. Taylor, and A. Pines, *Science* **271**, 1848 (1996).

<sup>4</sup>T. W. Kim, J. H. Lee, J. Choi, K. H. Kim, L. J. van Wilderen, L. Guerin, Y. Kim, Y. O. Jung, C. Yang, J. Kim, M. Wulff, J. J. van Thor, and H. Ihee, *J. Am. Chem. Soc.* **134**, 3145 (2012).

<sup>5</sup>M. J. Tucker, R. Oyola, and F. Gai, *J. Phys. Chem. B* **109**, 4788 (2005).

<sup>6</sup>R. M. Ballew, J. Sabelko, and M. Gruebele, *Proc. Natl. Acad. Sci. U. S. A.* **93**, 5759 (1996).

<sup>7</sup>F. Tani, N. Shirai, T. Onishi, F. Venelle, K. Yasumoto, and E. Doi, *Protein Sci.* **6**, 1491 (1997).

<sup>8</sup>S. Williams, T. P. Causgrove, R. Gilmanshin, K. S. Fang, R. H. Callender, W. H. Woodruff, and R. B. Dyer, *Biochemistry* **35**, 691 (1996).

<sup>9</sup>S. Yamada, N. D. B. Ford, G. E. Keller, W. C. Ford, H. B. Gray, and J. R. Winkler, *Proc. Natl. Acad. Sci. U. S. A.* **110**, 1606 (2013).

<sup>10</sup>R. H. Callender, R. B. Dyer, R. Gilmanshin, and W. H. Woodruff, *Annu. Rev. Phys. Chem.* **49**, 173 (1998).

<sup>11</sup>R. B. Dyer, F. Gai, and W. H. Woodruff, *Acc. Chem. Res.* **31**, 709 (1998).

<sup>12</sup>W. A. Eaton, V. Munoz, S. J. Hagen, G. S. Jas, L. J. Lapidus, E. R. Henry, and J. Hofrichter, *Annu. Rev. Biophys. Biomol. Struct.* **29**, 327 (2000).

<sup>13</sup>H. Li, H. M. Ke, G. P. Ren, X. G. Qiu, Y. X. Weng, and C. C. Wang, *Biophys. J.* **97**, 2811 (2009).

<sup>14</sup>S. Ke, M. C. Ho, N. Zhadin, H. Deng, and R. Callender, *J. Phys. Chem. B* **116**, 6166 (2012).

<sup>15</sup>S. S. Li, R. Wang, D. Y. Li, J. Ma, H. Li, X. C. He, Z. Y. Chang, and Y. X. Weng, *Sci. Rep.* **4**, 7 (2014).

<sup>16</sup>R. Koren and G. G. Hammes, *Biochemistry* **15**, 1165 (1976).

<sup>17</sup>N. Ferguson, J. Berriman, M. Petrovich, T. D. Sharpe, J. T. Finch, and A. R. Fersht, *Proc. Natl. Acad. Sci. U. S. A.* **100**, 9814 (2003).

<sup>18</sup>R. M. Ballew, J. Sabelko, C. Reiner, and M. Gruebele, *Rev. Sci. Instrum.* **67**, 3694 (1996).

<sup>19</sup>C. Y. Huang, Z. Getahun, Y. J. Zhu, J. W. Klemke, W. F. Degrad, and F. Gai, *Proc. Natl. Acad. Sci. U. S. A.* **99**, 2788 (2002).

<sup>20</sup>A. Troullier, D. Reinstadler, Y. Dupont, D. Naumann, and V. Forge, *Nat. Struct. Biol.* **7**, 78 (2000).

<sup>21</sup>X. L. Du, H. Frei, and S. H. Kim, *J. Biol. Chem.* **275**, 8492 (2000).

<sup>22</sup>R. Callender and R. B. Dyer, *Curr. Opin. Struct. Biol.* **12**, 628 (2002).

<sup>23</sup>M. Eigen and G. G. Hammes, *J. Am. Chem. Soc.* **82**, 5951 (1960).

<sup>24</sup>B. Nolting, *Biochem. Biophys. Res. Commun.* **227**, 903 (1996).

<sup>25</sup>E. F. Caldin and J. E. Crooks, *J. Sci. Instrum.* **44**, 449 (1967).

<sup>26</sup>I. Parker, *Proc. R. Soc. B* **237**, 379 (1989).

<sup>27</sup>J. Kubelka, *Photochem. Photobiol. Sci.* **8**, 499 (2009).

<sup>28</sup>C. Y. Huang, J. W. Klemke, Z. Getahun, W. F. DeGrado, and F. Gai, *J. Am. Chem. Soc.* **123**, 9235 (2001).

<sup>29</sup>R. Gilmanshin, S. Williams, R. H. Callender, W. H. Woodruff, and R. B. Dyer, *Proc. Natl. Acad. Sci. U. S. A.* **94**, 3709 (1997).

<sup>30</sup>M. Sadqi, L. J. Lapidus, and V. Munoz, *Proc. Natl. Acad. Sci. U. S. A.* **100**, 12117 (2003).

<sup>31</sup>G. Balakrishnan, Y. Hu, and T. G. Spiro, *Appl. Spectrosc.* **60**, 347 (2006).

<sup>32</sup>S. S. Sun, Ph.D. thesis, Institute of High Energy Physics, CAS, Beijing, China, 2013.

<sup>33</sup>J. J. Smith, J. A. McCray, M. G. Hibberd, and Y. E. Goldman, *Rev. Sci. Instrum.* **60**, 231 (1989).

<sup>34</sup>J. Hofrichter, *Methods Mol. Biol.* **168**, 159 (2001).

<sup>35</sup>M. P. Ye, Q. L. Zhang, H. Li, Y. X. Weng, W. C. Wang, and X. G. Qiu, *Biophys. J.* **93**, 2756 (2007).

<sup>36</sup>S. S. Li, Y. Y. Yu, D. Y. Li, X. C. He, Y. Z. Bao, and Y. X. Weng, *Chin. J. Chem. Phys.* **26**, 739 (2013).

<sup>37</sup>C. Krejtschi, R. Huang, T. A. Keiderling, and K. Hauser, *Vib. Spectrosc.* **48**, 1 (2008).

<sup>38</sup>C. M. Davis and R. B. Dyer, *Biochemistry* **53**, 5476 (2014).

<sup>39</sup>J. Wang and M. A. El-Sayed, *Biophys. J.* **76**, 2777 (1999).

<sup>40</sup>H. Ma, J. Ervin, and M. Gruebele, *Rev. Sci. Instrum.* **75**, 486 (2004).

<sup>41</sup>H. S. Chung, M. Khalil, A. W. Smith, and A. Tokmakoff, *Rev. Sci. Instrum.* **78**, 10 (2007).

<sup>42</sup>Q. L. Zhang, L. Wang, Y. X. Weng, X. G. Qiu, W. C. Wang, and J. X. Yan, *Chin. Phys. Lett.* **14**, 2484 (2005).

<sup>43</sup>L. Wang, X. W. Cai, J. W. Yang, X. Y. Wu, H. H. Jiang, and J. Y. Wang, *Opt. Lett.* **37**, 1986 (2012).

<sup>44</sup>W. O. Wray, T. Aida, and R. B. Dyer, *Appl. Phys. B: Lasers Opt.* **74**, 57 (2002).